

Glasslike vs. crystalline thermal conductivity in carrier-tuned $\text{Ba}_8\text{Ga}_{16}\text{X}_{30}$ clathrates ($\text{X} = \text{Ge}, \text{Sn}$)

M. A. Avila,¹ K. Suekuni,¹ K. Umeo,² H. Fukuoka,³ S. Yamanaka,³ and T. Takabatake^{1,4}

¹*Department of Quantum Matter, ADSM, Hiroshima University, Higashi-Hiroshima 739-8530, Japan*

²*N-BARD, Hiroshima University, Higashi-Hiroshima 739-8526, Japan*

³*Department of Applied Chemistry, Graduate School of Engineering, Hiroshima University, Higashi-Hiroshima 739-8527, Japan*

⁴*Institute for Advanced Materials Research, Hiroshima University, Higashi-Hiroshima 739-8530, Japan*

(Dated: June 18, 2018)

The present controversy over the origin of glasslike thermal conductivity observed in certain crystalline materials is addressed by studies on single-crystal x-ray diffraction, thermal conductivity $\kappa(T)$ and specific heat $C_p(T)$ of carrier-tuned $\text{Ba}_8\text{Ga}_{16}\text{X}_{30}$ ($\text{X} = \text{Ge}, \text{Sn}$) clathrates. These crystals show radically different low-temperature $\kappa(T)$ behaviors depending on whether their charge carriers are electrons or holes, displaying the usual crystalline peak in the former case and an anomalous glasslike plateau in the latter. In contrast, $C_p(T)$ above 4 K and the general structural properties are essentially insensitive to carrier tuning. We analyze these combined results within the framework of a Tunneling/Resonant/Rayleigh scatterings model, and conclude that the evolution from crystalline to glasslike $\kappa(T)$ is accompanied by an increase both in the effective density of tunnelling states and in the resonant scattering level, while neither one of these contributions can solely account for the observed changes in the full temperature range. This suggests that the most relevant factor which determines crystalline or glasslike behavior is the coupling strength between the guest vibrational modes and the frameworks with different charge carriers.

I. INTRODUCTION

The understanding of thermal conductivity behavior $\kappa(T)$ is of direct interest to any research involving the discovery, design and development of materials for thermoelectric conversion applications, where $\kappa(T)$ should be as small as possible, while at the same time thermopower $S(T)$ and electrical conductivity $\sigma(T)$ should be large. In the semiclassical theory for electron and phonon transport,^{1,2} several mechanisms are known as contributors to heat conduction/phonon scattering in a material, consequently affecting its overall thermal conductivity.

In metals, heat conduction by charge carriers is the largest contribution, and is well described by the Wiedemann-Franz law $\kappa_c = L\sigma T$, which directly relates the carrier thermal conductivity κ_c with an appropriate Lorentz number $L \sim 2 - 3 \times 10^{-8} \text{ W}\Omega/\text{K}^2$, the electrical conductivity σ and the temperature T . Due to their typically large charge carrier densities n_c , metals have large $\sigma(n_c, T)$ and thus large κ_c in the range of 50–500 W/m K at room temperature.

Conversely, semi-metallic, semi-conducting and insulating compounds have low n_c and $\sigma(T)$, therefore small and often negligible $\kappa_c(T)$ and the overall heat conduction behavior $\kappa(T)$ near room temperature is in the range of 10 – 50 W/m K, governed mostly by contributions $\kappa_L(T)$ arising from the crystal lattice. At $T \rightarrow 0$, $\kappa(T) \rightarrow 0$ from basic thermodynamic principles, so within the first few Kelvins $\kappa(T)$ increases quickly as a power law T^r , with $1 \leq r \leq 3$ depending on which phonon scattering mechanisms dominate at low temperatures. At higher temperatures the phonon scattering is generally described as governed mostly by umklapp

processes, for which the Debye approximation approach shows a decrease with a T^{-1} dependence. Therefore, at some intermediate temperature usually around 10–50 K, a characteristic “crystalline peak” is observed in $\kappa(T)$ for common compounds, due to the crossover from one regime to another.²

The peak usually appears equally in polycrystalline materials since grain boundary scattering is in general a minor contribution,^{2,3} unless the average grain size becomes very small or the temperature very low. However, glasses are an exception to the above because of two basic factors: the very low mean free path for both electrons and phonons, and the presence of low-energy tunnelling states (TS), i.e., different localized potential minima for atomic positions in their amorphous distribution of nuclei.² This class of materials shows extremely low heat conduction and a universal behavior of $\kappa(T)$: the lowest temperature behavior (up to ~ 1 K) rises as T^2 due to scattering by the tunnelling states, then levels off as a characteristic intermediate temperature plateau (attributed to Rayleigh scattering). Above ~ 20 K it resumes a slow increase, until roughly levelling off again at higher temperatures.

In more recent years, the search for new and potentially useful thermoelectric materials^{4,5} has led to the discovery of compounds that not only have unusually low thermal conductivity, but whose general behavior resembles that of a glassy material despite the fact that they are true (albeit disordered) crystalline lattices.⁶ A prominent example is the intermetallic compound $\text{Sr}_8\text{Ga}_{16}\text{Ge}_{30}$, with a filled type-I clathrate structure⁷ (6 larger X_{24} cages forming tetrakaidecahedra plus 2 smaller X_{20} cages forming dodecahedra, see Fig. 1) for which $\kappa(T)$ was first measured by Nolas *et al.* in 1998.³ A model was proposed⁸

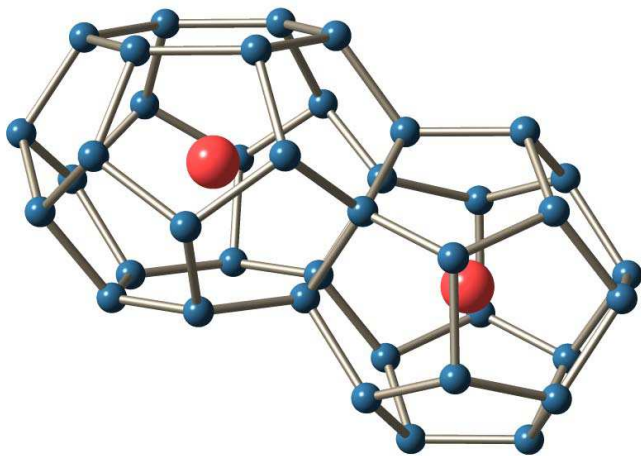


FIG. 1: (Color online) The two cages of the type-I clathrate structure adopted by $\text{Ba}_8\text{Ga}_{16}\text{Ge}_{30}$. If we consider the cage “construction unit” as 4 atoms connected in zig-zag from top to bottom, then the larger X_{24} cage (left) is made of 6 such units and the smaller X_{20} cage (right) is made of 5 units.

to explain this material’s glasslike behavior, based on the idea that TS exist for the Sr(2) guest ion in the X_{24} cage,⁹ to which it is rather loosely bound because of an ion-to-cage size mismatch. A combination of phonon scattering by TS, resonant scattering on large, Einstein-like localized vibration modes (guest *rattling*) and Rayleigh scattering was used to adequately reproduce the experimental $\kappa(T)$ behavior (henceforth we will refer to this combination as the TRR model). Later investigations amply demonstrated a splitting of the Sr(2) site into four off-center positions,^{10,11,12} among which the ions could indeed tunnel.

As other clathrate compounds started being investigated, the TRR model was challenged by at least two other models. One proposes that the tunnelling states are not required, only an *off-center* vibration of the guest ions,^{13,14} and another proposes that the guest ions don’t play a major role at all at low temperatures, but rather it is the phonon scattering on charge carriers that leads to the glasslike behavior.^{15,16,17,18}

In this work we address the issue by performing single crystal x-ray diffraction (SCXRD), thermal conductivity $\kappa(T)$ and heat capacity $C_p(T)$ experiments on $\text{Ba}_8\text{Ga}_{16}\text{Sn}_{30}$ (BGS) and $\text{Ba}_8\text{Ga}_{16}\text{Ge}_{30}$ (BGG) crystals, which have been tuned through the crystal growth process to display n-type or p-type majority charge carriers as a result of small imbalances in their Ga:Ge or Ga:Sn ratios.^{19,20} By analyzing the differences and similarities between the behaviors of these samples, we can test the applicability of the various models proposed to explain the origin of unusual glasslike behavior, in this case observed for p-type samples whereas the n-type samples show the normal crystalline peak.

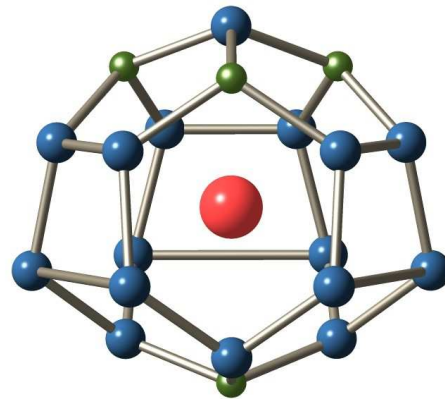


FIG. 2: (Color online) Irregular cage of the type-VIII clathrate structure adopted by $\text{Ba}_8\text{Ga}_{16}\text{Sn}_{30}$. The four smaller cage spheres represent the $8c$ site, preferentially occupied by Ga atoms.

TABLE I: Average Ba:Ga:X content (X = Ge, Sn) in the four measured crystals as determined by electron-probe microanalysis.

Sample Name	Starting Flux Composition	Crystal Composition
n-BGS	8 : 16 : 60	8.0 : 15.98 : 30.02
n-BGG	8 : 38 : 34	8.0 : 15.94 : 30.06
p-BGS	8 : 38 : 30	8.0 : 16.14 : 29.86
p-BGG	8 : 38 : 30	8.0 : 16.10 : 29.90

II. EXPERIMENTAL DETAILS

Growth details of the batches used in this work are described in previous papers.^{19,20,21} Single crystalline polyhedrons of 3-10 mm in diameter were obtained by a self-flux method. The carrier type is tuned by choosing Ga or Sn flux¹⁹ in the case of BGS or by adjusting the relative Ge content in the initial mix with Ga flux²⁰ in the case of BGG. The batch name, flux composition and crystal composition determined by a JEOL JXA-8200 electron-probe microanalyzer (EPMA) are summarized in table I. The composition values are averages over 10 regions of each crystal, although there are random fluctuations of up to ± 0.1 throughout the crystals. The values shown for the p-BGG sample should be considered a correction to those published in refs. 20 and 22, since this was a more careful evaluation made on the same batch. As expected from charge balance principles, Ga-rich samples show p-type carriers while Ge-rich samples show n-type carriers.

Thermal conductivity experiments were performed using a steady-state method on home-made systems, in the range of 0.3-300 K (BGG) and 4-300 K (BGS), although reliable data is only obtainable up to about 150 K. At higher temperatures, thermal losses by radiation and wire conduction prevent the correct measurement of the intrinsic sample properties. The electronic contribution

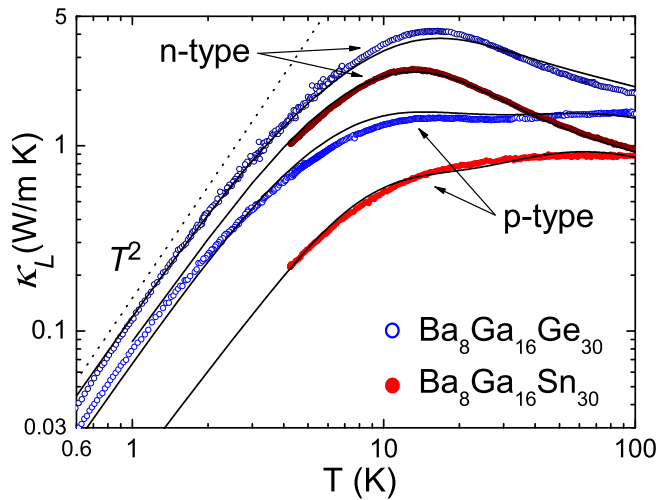


FIG. 3: (Color online) Temperature dependence of the thermal conductivity of $\text{Ba}_8\text{Ga}_{16}\text{Ge}_{30}$ and $\text{Ba}_8\text{Ga}_{16}\text{Sn}_{30}$ with different carrier types. Solid lines are best fits of the TRR model as described in the Discussion section.

$\kappa_c(T)$ of all samples estimated by the Wiedeman-Franz law is negligible up to 100 K, so the measured $\kappa(T)$ is equated to the lattice contribution $\kappa_L(T)$. Heat capacity was measured using a Quantum Design PPMS with its standard thermal-relaxation method, in the range $0.4 \leq T \leq 300$ K.

For SCXRD experiments, broken pieces of n-BGS and p-BGS with approximate dimensions of $0.1 \times 0.1 \times 0.1$ mm³ were selected. The diffraction data were collected with a Rigaku R-AXIS RAPID imaging plate area detector using graphite-monochromated Mo K_α radiation. Refinements were performed using the CrystalStructure²³ software. Structures were solved by direct methods and expanded using Fourier techniques. All sites were assumed to be fully occupied.

III. EXPERIMENTAL RESULTS

A. Thermal Conductivity

The lattice thermal conductivity $\kappa_L(T)$ of all four samples is shown in Fig. 3 (symbols are the as-measured experimental data points and solid lines represent fits to the data by the TRR model which will be detailed in the Discussion section). At 100 K and above (not shown), $\kappa_L(T)$ for BGS is roughly half that of BGG (about 1 and 2 W/m K respectively). This can be understood as a consequence of three main factors: (i) if the rattling of the guest ions is the main contributor to the unusually high phonon scattering level in these materials,²⁴ the larger cage size in BGS leads to larger rattling of the guest ions; (ii) in the BGS unit cell all 8 guest ions vibrate with equal intensity (single crystallographic site for Ba in the Type-VIII clathrate structure), while in BGG only

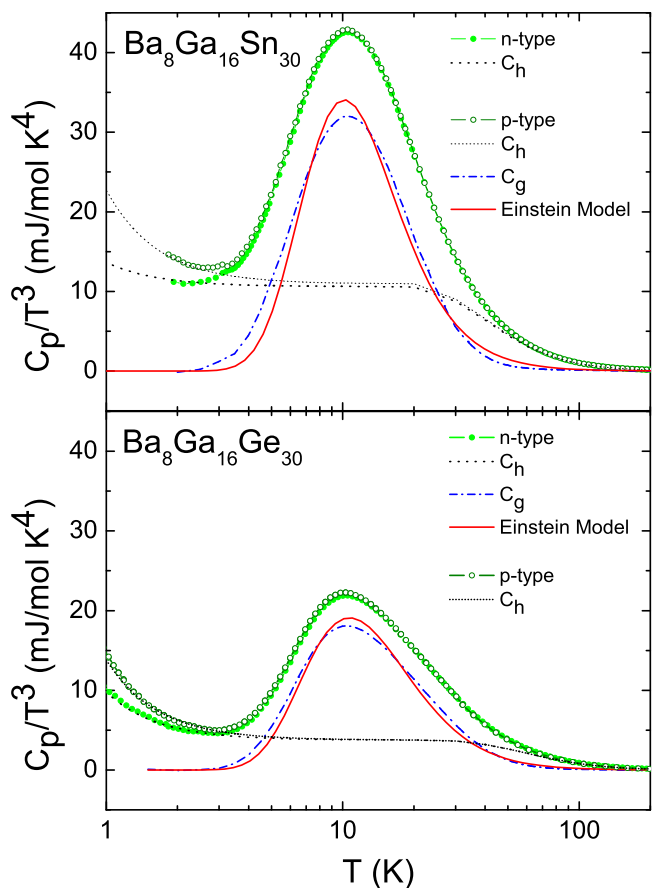


FIG. 4: (Color online) Heat capacity C_p of $\text{Ba}_8\text{Ga}_{16}\text{Sn}_{30}$ and $\text{Ba}_8\text{Ga}_{16}\text{Ge}_{30}$ with different carrier types, presented as C_p/T^3 vs. T . Solid lines are best fits of the Einstein model as described in the Discussion section.

the 6 guest ions inside the X_{24} cages show large rattling; and (iii) the heavier Sn atoms produce lower frequency phonons, which are more easily scattered.

Below 100 K, each sample behaves quite differently, depending more on the carrier type than on the compound. The two n-type samples increase towards a peak, while the p-type samples remain at a plateau, smaller by a factor of 3 – 4 in value than the n-type counterparts near the peak. Below 10 K, $\kappa_L(T)$ for all samples decreases fast and, in the case of BGG which was measured to lower temperatures, a gradual crossover to a T^2 regime is clearly observed. This implies a phonon mean free path inversely proportional to frequency⁸ which is the expected dependence when phonon scattering by tunnelling states is dominant. The T^2 behavior contrasts with a previously reported result showing a $T^{1.5}$ dependence for p-type BGG.¹⁵

B. Heat Capacity

The data points in Figs. 4a and 4b show the as-measured specific heats $C_p(T)$ for the BGS and BGG

TABLE II: Summary of crystallographic parameters from the structural refinement of a n-type $\text{Ba}_8\text{Ga}_{16}\text{Sn}_{30}$ single crystal. Space group $I43n$ (No. 217), $a = 11.586(1)$ Å, $Z = 1$, $R = 0.009$, $R_w = 0.009$, $B_{eq} = (8\pi^2/3) \sum_i \sum_j U_{ij} a_i^* a_j^* a_i a_j$.

Atom	site	x	y	z	B_{eq} (Å ²)	occupancy
Ba(1)	8c	0.68490(5)	0.31510(5)	0.31510(5)	3.32(1)	1
Ga(1) / Sn(1)	12d	0.5000	0.0000	0.2500	1.65(1)	0.184(12) / 0.816(12)
Ga(2) / Sn(2)	2a	0.5000	0.5000	0.5000	0.97(2)	0.158(22) / 0.842(22)
Ga(3) / Sn(3)	24g	0.41549(4)	0.14887(4)	0.41549(4)	1.333(9)	0.314(8) / 0.686(8)
Ga(4) / Sn(4)	8c	0.36558(6)	0.36558(6)	0.36558(6)	1.07(2)	0.766(12) / 0.234(12)

TABLE III: Summary of crystallographic parameters from the structural refinement of a p-type $\text{Ba}_8\text{Ga}_{16}\text{Sn}_{30}$ single crystal. Space group $I43n$ (No. 217), $a = 11.587(1)$ Å, $Z = 1$, $R = 0.0218$, $R_w = 0.0157$, $B_{eq} = (8\pi^2/3) \sum_i \sum_j U_{ij} a_i^* a_j^* a_i a_j$.

Atom	site	x	y	z	B_{eq} (Å ²)	occupancy
Ba(1)	8c	0.68507(8)	0.31493(8)	0.31493(8)	3.25(2)	1
Ga(1) / Sn(1)	12d	0.5000	0.0000	0.2500	1.69(2)	0.152(16) / 0.848(16)
Ga(2) / Sn(2)	2a	0.5000	0.5000	0.5000	0.90(3)	0.233(26) / 0.767(26)
Ga(3) / Sn(3)	24g	0.41565(4)	0.14836(4)	0.41565(4)	1.308(14)	0.318(10) / 0.682(10)
Ga(4) / Sn(4)	8c	0.36577(6)	0.36577(6)	0.36577(6)	1.077(14)	0.707(12) / 0.293(12)

samples respectively, plotted as C_p/T^3 vs. T . This plotting style emphasizes the contributions of localized vibrations of guest atoms (Einstein oscillators), which appear as pronounced peaks over a “background” contribution of a Debye solid. For these samples, the charge carrier contribution is negligible above ~ 4 K, but responsible for the T^{-2} upward curvature upon cooling below this temperature. A more traditional plot of C_p/T vs. T^2 below 4 K (not shown) is used to estimate with good accuracy the Sommerfeld coefficient γ of the charge carriers and the Debye temperature Θ_D of the 46 framework atoms, and then subtract the host contribution C_h (dotted lines) in order to isolate the Einstein-like contribution C_g of the guest ions (dash-dotted peak).

Contrary to the heat transport data, in both BGS and BGG the heat capacity data show the same behavior above ~ 4 K for different carrier types. This result demonstrates there is no fundamental change in the entropic properties of these compounds within the range of deviations from stoichiometry studied. If the rattling behavior of the guest ion is not significantly changed for different carrier types in the framework, then it should be the coupling between the guest vibration and the frameworks with different carriers that changes. In other words, frameworks with holes have their phonon modes more effectively scattered by the Ba vibration than those with electrons.

C. Single-Crystal X-Ray Diffraction

Tables II and III summarize the refinement results made for room temperature SCXRD data of n-BGS and p-BGS respectively. The anomalously large isotropic thermal parameter B_{eq} of the Ba site compared to the Ga/Sn sites is a signature of the enhanced vibration (rat-

ting) of the guest ion in the oversized cage, however, no relevant difference is observed between the crystals.

The resulting sets of data do not allow a detailed composition analysis for comparison with EPMA results, because the R factor was insensitive to occupation probability within deviations of ± 0.2 from stoichiometry, but the framework sites show consistent preferential occupations for Sn(1) and Sn(2) in the respective 12d and 2a crystallographic sites, while Ga(4) has the preferential occupation of the 8c site (in accordance with the idea that the smaller Ga atom should more easily occupy the site with smaller bond distances between neighbors) and the 24g site remains more randomly occupied by Sn(3) and Ga(3). This is true for crystals with both types of carriers, the only consistent and relevant difference we could find in these refinements was a larger relative occupation of the 2a site by Ga(2) for the p-BGS samples (the top atom in Fig. 2). This could be where the “extra” Ga ions prefer to enter in Ga-rich samples, but whether or not this can have any influence on the overall guest/framework coupling would require more detailed investigation.

IV. DISCUSSION

We now present and discuss the models used to analyze the data in Figs. 3 and 4. The specific heat is expressed as a sum of 3 main contributions:

$$C_p = C_c + C_D + C_E, \quad (1)$$

where $C_c = \gamma T$ is the electronic specific heat of the charge carriers,

$$C_D = \frac{12\pi^4 N_D k_B}{5} \int_0^{\Theta_D/T} \frac{x^4 e^x dx}{(e^x - 1)^2} \quad (2)$$

with $x = \hbar ck/k_B T$ is the Debye model for the lattice specific heat of N_D Debye oscillators per unit cell, whose numerical solution can be found in Solid State Physics textbooks, and

$$C_{Ei} = \sum_i p_i N_{Ei} R \left(\frac{\Theta_{Ei}}{T} \right)^2 \frac{e^{\Theta_{Ei}/T}}{(e^{\Theta_{Ei}/T} - 1)^2} \quad (3)$$

is the Einstein specific heat of the i -th vibrational mode of any existing rattling ions. For our analysis we assume that the 8 rattling guest ions are sufficiently decoupled from the 46 rigid framework atoms, so that we can make the association $C_g = C_{Ei}$ and $C_h = C_c + C_D$ respectively.

The solid line in Fig. 4a indicates the best fit of eq. 3 to the isolated Einstein contribution in p-BGS. It is important to emphasize that in this analysis for the type-VIII structure, the dimensionality and the number of Einstein oscillators are fixed at $p = 3$ and $N_E = 8$ so there is a *single* fitting parameter Θ_E for BGS, which alone governs all the peak characteristics - position, height and width. The fact that the best fitted curve with $\Theta_E = 49.9$ K so closely reproduces the experimental peak in all these aspects is a solid testimony to how successful the Einstein model is in describing the vibrational behavior of the 8 Ba ions in this compound. The data is actually slightly broadened with respect to the model, which may be the result of a narrow distribution of Θ_E around the mean value (a consequence of Ga/Sn site disorder), and/or a slightly anisotropic vibration of each guest ion in its respective irregular cage (resembling an ovoid with diameter varying between 7.3 – 8.2 Å, see Fig. 2). We will see next how anisotropic vibration plays a much more important role in the BGG compound.

Contrary to BGS, the specific heat of BGG *cannot* be adequately fit with a single Θ_E and $N_E = 8$. If N_E is freed as a fitting parameter, the best fit naturally decreases this to $N_E = 6.1$ (and $\Theta_E = 55$ K), consistent with the fact that the 6 Ba(2) ions in the larger X_{24} cages are the main rattlers, but the fitting quality is still not satisfactory. Until now, the usual approach^{15,22} to analyze the heat capacity of BGG has been to assign two different Einstein contributions ($i = 2$ in Eq. 3). This results in excellent fits with $\Theta_{E1} = 70 - 80$ K and $\Theta_{E2} = 30 - 40$ K. However, the *number* of Einstein oscillators N_{E1} and N_{E2} results opposite to what one would expect if these numbers were to represent the two Ba sites, i.e., there is a greater number of Ba oscillators with larger Θ_{E1} ($N_{E1} = 6 - 9$) than those with smaller Θ_{E2} ($N_{E2} = 1.5 - 2.0$). This is difficult to physically justify, since larger rattling implies *smaller* Θ_E .

We offer an analysis which better reconciles with the guest ions' known physical properties. The starting point is that, due to the X_{24} cage shape (Fig. 1, left), the Ba(2) ions show a strongly *anisotropic* vibration with greater amplitude within the plane parallel to the cage's two hexagons.⁹ Because the dimensionality p plays a role

in the Einstein model (see Eq. 3), at least two vibrational modes should be required to describe the Ba(2) site alone: in-plane (Θ_{E2}^{\parallel}) and out-of-plane (Θ_{E2}^{\perp}) respectively. In addition, a third vibrational mode (Θ_{E1}) is required to account for the smaller, but still Einstein-like, rattling of the two Ba(1) site ions in the X_{20} dodecahedra (Fig. 1, right), which can be assumed isotropic.¹¹ In this model, the dimensionalities and numbers of oscillators are predefined: $p_1 N_{E1} = 3 \times 2$, $p_2^{\parallel} N_{E2}^{\parallel} = 2 \times 6$, $p_2^{\perp} N_{E2}^{\perp} = 1 \times 6$, so the fitting parameters are only the three Einstein temperatures, with the additional constraint that $\Theta_{E2}^{\parallel} < \Theta_{E2}^{\perp}, \Theta_{E1}$. The best fitting of this model results in $\Theta_{E1} = 87.2$ K, $\Theta_{E2}^{\parallel} = 49.4$ K and $\Theta_{E2}^{\perp} = 87.1$ K. The similarity between Θ_{E2}^{\parallel} of BGG and Θ_E of BGS is reasonable, since the largest diameters of both cages are essentially the same (~ 8.2 Å). The similarity between Θ_{E2}^{\perp} and Θ_{E1} in BGG is also reasonable since the X_{24} cage size in the out-of-plane direction is very close to the X_{20} cage size (~ 5.5 Å). This means a further simplification can be made in the model by assuming only two parameters Θ_{E1} and Θ_{E2} with $p_1 N_{E1} = p_2 N_{E2} = 12$, where Θ_{E1} represents the 3D vibration of the Ba(1) ions and the 1D out-of-plane vibration of the Ba(2) ions; while Θ_{E2} represents the larger, 2D in-plane vibration of the Ba(2) ions. This results in the solid curve shown in Fig. 4b and, as with BGS, the data for BGG is only slightly broadened with respect to the model.

With the heat capacity parameters determined, we now analyze the lattice thermal conductivity κ_L of all samples, using the same procedure applied previously for analysis of the n-BGS sample,²¹ which is in turn based on the TRR model initially used in ref. 8 to describe $\text{Sr}_8\text{Ga}_{16}\text{Ge}_{30}$. In the semi-classical theory, κ_L is given by

$$\kappa_L = \frac{1}{3} \int_0^{\omega_D} d\omega [C_L(\omega, T) v l], \quad (4)$$

where $C_L(\omega, T)$ is the phonon specific heat, ω_D is the Debye frequency, v is the average sound velocity and l is the phonon mean free path, which must be averaged over all major contributing scattering mechanisms. Thus, in the TRR model it is written as

$$l = (l_{TS}^{-1} + l_{Res}^{-1} + l_{Ray}^{-1})^{-1} + l_{min}. \quad (5)$$

The low-energy excitations of the guest ions tunnelling between localized states scatter phonons as

$$l_{TS}^{-1} = A \left(\frac{\hbar\omega}{k_B} \right) \tanh \left(\frac{\hbar\omega}{2k_B T} \right) + \frac{A}{2} \left(\frac{k_B}{\hbar\omega} + \frac{1}{BT^3} \right)^{-1}, \quad (6)$$

where A and B are microscopic parameters describing the tunnelling states characteristics.²⁵ At higher energies,

TABLE IV: Parameters used to generate the solid line curves in Figs. 3 and 4, which best fit the respective experimental data set for lattice thermal conductivity and specific heat. See text for detailed descriptions.

Symbol	Unit	n-BGG	p-BGG	n-BGS	p-BGS
A	$10^4/(\text{m K})$	1.4	2.5	2.5	17
B	$1/\text{K}^2$	0.1	0.1	0.1	0.1
A/B	10^5K/m	1.4	2.5	2.5	17
C_1	$1/(\text{m s}^2 \text{K}^2)$	0.2	2.0	0.7	5.0
Θ_{E1}	K	87	87	50	50
Γ_1		0.5	1.5	0.4	1.5
C_2	$1/(\text{m s}^2 \text{K}^2)$	0.2	2.0	-	-
Θ_{E2}	K	49 ^a	49 ^a	-	-
Γ_2		0.5	1.5	-	-
D	K^4/m	0.85	0.5	2.8	1.7
γ	$\text{mJ}/(\text{mol K}^2)$	6	9	1.3	11
Θ_D	K	288	288	200	200
ν	m/s	2898	2898	2250	2250

^aTwo-dimensional vibration (see text).

phonons are scattered through a resonance effect against guest ion rattling as:

$$l_{Res}^{-1} = \sum_i \frac{C_i \omega^2 T^2}{(\omega_i^2 - \omega^2)^2 + \Gamma_i \omega_i^2 \omega^2}, \quad (7)$$

where C_i and Γ_i are phenomenological parameters related to a simple mechanical oscillator.²⁶ We also need to include the empirical but always present, frequency-only dependent Rayleigh scattering

$$l_{Ray}^{-1} = D \left(\frac{\hbar \omega^4}{k_B} \right), \quad (8)$$

and finally the last term $l_{min} = 1 \text{ \AA}$ is the cut-off limit.

Results from the best fits of the data shown in Figs. 3 and 4 are summarized in Table IV. The most relevant results in terms of comparing the p-type with n-type samples are the increase in the resonant scattering level (C_i), and in the TS scattering level. The latter can be expressed by the ratio $A/B = \tilde{n}(\hbar v)^2/\pi k_B$, which in glasses is essentially a measure of the *subset* density of tunnelling states \tilde{n} that are able to strongly couple to the phonons and effectively scatter them.²⁵ Therefore, the increase in A/B observed upon changing from n-type to p-type cages does not necessarily mean the total density of TS has increased, only that the existing states are more effectively coupled.

An interesting exercise can be made to help understand the influence of these different contributions in the TRR model. If we begin with the fitting results for $\kappa_L(T)$ of the n-type samples, it is impossible to fit the respective p-type $\kappa_L(T)$ by increasing the intensity of only one of these contributions (TS or resonant). The TS are mainly responsible for decreasing the low-temperature $\kappa_L(T)$ up to the first few Kelvins, and by itself the TS contribution

is incapable of changing the peak into a plateau. Conversely, an increase in the resonant scattering level (based on *fixed* values of $\Theta_E = 50 \text{ K}$ from heat capacity and increased phenomenological coupling strength parameters C_i), readily brings the peak down to a plateau/dip, but quickly loses its ability to follow the $\kappa_L(T)$ drop below about 10 K. Therefore, we may conclude that the TRR model adequately reproduces the entire range of $\kappa_L(T)$ for all samples up to 100 K, provided that the coupling of the framework phonons with the guest ion tunnelling *and* rattling is increased in p-type samples.

Let us now focus on some other proposals regarding candidate mechanisms for glasslike behavior in clathrates, which challenge the TRR model. First: is the presence of tunnelling states really necessary, or is *off-center* vibration a sufficient mechanism? The question was raised by Bridges and Downward¹³ primarily based on the existing data at the time, where Sr and Eu guests clearly show off-center sites^{10,11,12} and glasslike $\kappa(T)$, while Ba guests appear to show *on-center* vibration^{10,11,12} (within experimental resolution) and a crystalline peak. Later studies demonstrated glasslike behavior for p-type BGG^{15,20} and now for p-type BGS (this work), so this argument by itself is no longer valid, unless a closer look at the Ba vibration in these compounds through microscopic techniques shows that off-center vibration modes do exist for p-type samples (even if much smaller than for Sr and Eu guests) but not for n-type samples. Raman scattering and EXAFS studies are presently being conducted on our carrier-tuned BGG crystals, which may help clarify this issue. Still, good arguments were made by the authors in terms of describing how off-center vibration does indeed help enhance the *coupling* between guest vibration modes and the framework phonons.^{13,14}

A second challenge to the TRR model is: can the shift from crystalline to glasslike behavior be explained solely by phonon scattering mechanisms within the framework, i.e., by interactions between phonons and charge carriers? This question was raised in a series of papers by Bentien *et al.*^{15,16,18} which we now discuss.

The first work¹⁵ called attention to an observed $\kappa(T) \propto T^{1.5}$ dependence at low-temperature for p-BGG and a kink in their data at about 2 K (neither of which were reproduced with our crystals). They also pointed out that the phonon-charge carrier mechanism could not explain the lowering of $\kappa_L(T)$ above $\sim 15 \text{ K}$, so the resonant scattering on the guest vibration was once again invoked, but to account for only the differences above 15 K. The second work¹⁶ compared several polycrystalline samples of type-VIII and type-I $\text{Eu}_8\text{Ga}_{16}\text{Ge}_{30}$ (α -EGG and β -EGG respectively,²⁷ all with n-type carriers), clearly demonstrating that β -EGG shows glasslike $\kappa_L(T)$ while α -EGG does not. The difference was interpreted in terms of changes in the band structure, with a much enhanced effective mass m^* found in β -EGG. However, the cage sizes and shapes are also quite different between these two structures. The type-I X_{24} cages are essentially the

same size for all Ge clathrates ($5.5 \times 8.2 \text{ \AA}$, see Fig. 1) but the type-VIII cage in α -EGG ($6.7 \times 7.5 \text{ \AA}$ ovoid similar to Fig. 2) is significantly smaller than that of BGS, so any change in $\kappa_L(T)$ can also be argued or modelled in terms of changes in the Eu vibration modes and their coupling to the framework. Unfortunately α -EGG samples with p-type carriers are as yet unavailable, but it wouldn't be surprising if they showed glasslike $\kappa_L(T)$ as we found in p-BGS. The third and more recent work¹⁸ shows results for $\text{Ba}_8\text{Ni}_x\text{Ge}_{46-x}$ similar to what we have obtained here for BGG and BGS, therefore the same analysis and discussion we have conducted here can also be applied to those results.

Still, it is obvious that the influence of charge-carriers cannot be neglected with respect to their density n_c , effective mass m^* , electronic mean free path l_c , etc. It is quite clear from our measurements and all previously reported data on Ba-filled clathrates, that the p-type carriers are playing a relevant role in producing an increased phonon scattering in these compounds, which we view as yet another additional factor capable of contributing to lower $\kappa_L(T)$, possibly through direct interaction with the phonons, but especially by mediating an enhanced coupling of these with the guest vibration modes. A few brief examples for such mediation possibilities are: 1) n-type frameworks could allow a greater degree of *coherence* in the vibrations of neighboring Ba guests than p-type frameworks, which would lead to larger mean free paths and less effective scattering; 2) Since the type and density of charge carriers result from stoichiometry imbalances, they may affect the framework rigidity at certain sites, and therefore how easily it can couple with the rattler ions.

V. CONCLUSION

We have succeeded in growing large single crystals of $\text{Ba}_8\text{Ga}_{16}\text{Sn}_{30}$ and $\text{Ba}_8\text{Ga}_{16}\text{Ge}_{30}$ with both n-type and p-type majority carriers, and found that these compounds show low temperature lattice thermal conductivity behavior strongly dependent on the carrier type. A shift from crystalline to glasslike behavior is observed for both compounds when changing the majority carriers from n-type to p-type through composition tuning. These differences can be mostly reproduced by an increase in resonant scattering, however, an increase in both resonant and tunnelling scattering levels are required to reproduce the full set of data below 100 K. Heat capacity

and single-crystal x-ray diffraction data indicated that these increases are not the result of any major change in the guest ions' vibrational behaviors, therefore a more effective coupling of the frameworks with p-type carriers to the TS and rattling vibrations of the guest ions is the most likely mechanism. The T^2 dependence in $\kappa_L(T)$ obtained at lowest temperatures for both n-type and p-type $\text{Ba}_8\text{Ga}_{16}\text{Ge}_{30}$ indicates that tunnelling states should be present for the Ba(2) ions in this compound, therefore its mere presence is insufficient to guarantee glasslike $\kappa_L(T)$.

In fact, our results indicate that the various proposed mechanisms which may lead to glasslike behavior are all partially correct and at the same time incomplete. The general scenario that we see emerging can indeed be expressed as: *it's all about the coupling*. For reasons that still need to be explained microscopically, the n-type frameworks are more weakly coupled to the guest vibration modes than the p-type frameworks. Thus, the Ba ions' smaller and (almost?) on-center vibration is not coupled strongly enough to the n-type framework phonons to produce the glasslike behavior, but the p-type framework crosses the necessary coupling strength threshold to achieve this scattering regime. In contrast, Sr and Eu ions in the type-I Ge clathrates have clearly off-center and larger rattling, capable of a strong enough coupling even with the n-type frameworks to produce glasslike behavior (no p-type frameworks have been reported yet for these compounds). In a series of carefully tuned Ba-based clathrates it should be possible to observe a continuous transition from glasslike to crystalline $\kappa_L(T)$. Likewise, in a series of n-type (Sr,Eu)-based clathrates the same continuous transition should be observed not from carrier tuning, but from a physical or chemical reduction of cage size to dampen the off-center vibration level.

Acknowledgments

We thank M. Udagawa, F. Bridges and D. Huo for fruitful discussions, and Y. Shibata for the EPMA analysis. Specific heat and thermal conductivity measurements were carried out at Natural Science Center for Basic Research and Development (N-BARD) Hiroshima University. This work was financially supported by the Grants in Aid for Scientific Research(A) (No. 18204032), the COE Research (13CE2002) and the priority area "Skutterudite" (No. 15072205) from MEXT, Japan.

¹ J. M. Ziman, *Electrons and Phonons* (Oxford University Press, 1960).

² T. M. Tritt, ed., *Thermal Conductivity* (Kluwer Academic/Plenum Publishers, New York, 2004).

³ G. S. Nolas, J. L. Cohn, G. A. Slack, and S. B. Schujman, *Appl. Phys. Lett.* **73**, 178 (1998).

⁴ C. Wood, *Rep. Prog. Phys.* **51**, 459 (1988).

⁵ G. A. Slack, in *CRC Handbook of Thermoelectrics* (Chemical Rubber, Boca Raton, FL, 1995), chap. 34, p. 407.

⁶ D. G. Cahill, S. K. Watson, and R. O. Pohl, *Phys. Rev. B* **46**, 6131 (1992).

⁷ B. Eisenmann, H. Schafer, and R. Zagler, *J. Less-Common*

- Met. **118**, 43 (1986).
- ⁸ J. L. Cohn, G. S. Nolas, V. Fessatidis, T. H. Metcalf, and G. A. Slack, Phys. Rev. Lett. **82**, 779 (1999).
- ⁹ G. S. Nolas, T. J. R. Weakley, J. L. Cohn, and R. Sharma, Phys. Rev. B **61**, 3845 (2000).
- ¹⁰ B. C. Chakoumakos, B. C. Sales, D. G. Mandrus, and G. S. Nolas, J. Alloys. Comp. **296**, 80 (2000).
- ¹¹ B. C. Sales, B. C. Chakoumakos, R. Jin, J. R. Thompson, and D. Mandrus, Phys. Rev. B **63**, 245113 (2001).
- ¹² I. Zerec, V. Keppens, M. A. McGuire, D. Mandrus, B. C. Sales, and P. Thalmeier, Phys. Rev. Lett. **92**, 185502 (2004).
- ¹³ F. Bridges and L. Downward, Phys. Rev. B **70**, 140201(R) (2004).
- ¹⁴ R. Baumbach, F. Bridges, L. Downward, D. Cao, P. Chesler, and B. Sales, Phys. Rev. B **71**, 024202 (2005).
- ¹⁵ A. Bentien, M. Christensen, J. D. Bryan, A. Sanchez, S. Paschen, F. Steglich, G. D. Stucky, and B. B. Iversen, Phys. Rev. B **69**, 045107 (2004).
- ¹⁶ A. Bentien, V. Pacheco, S. Paschen, Y. Grin, and F. Steglich, Phys. Rev. B **71**, 165206 (2005).
- ¹⁷ V. Pacheco, A. Bentien, W. Carrillo-Cabrera, S. Paschen, F. Steglich, and Y. Grin, Phys. Rev. B **71**, 165205 (2005).
- ¹⁸ A. Bentien, S. Johnsen, and B. B. Iversen, Phys. Rev. B **73**, 094301 (2006).
- ¹⁹ M. A. Avila, D. Huo, T. Sakata, K. Suekuni, and T. Takabatake, J. Phys.: Condens. Matter **18**, 1585 (2006).
- ²⁰ M. A. Avila, K. Suekuni, K. Umeo, and T. Takabatake, Physica B (in press).
- ²¹ D. Huo, T. Sakata, T. Sasakawa, M. A. Avila, M. Tsubota, F. Iga, H. Fukuoka, S. Yamanaka, S. Aoyagi, and T. Takabatake, Phys. Rev. B **71**, 075113 (2005).
- ²² K. Umeo, M. A. Avila, T. Sakata, K. Suekuni, and T. Takabatake, J. Phys. Soc. Jpn. **74**, 2145 (2005).
- ²³ CrystalStructure 3.10 and 3.7.0 : Crystal Structure and Analysis Package, Rigaku and Rigaku/MSC (2000-2005). 9009 New Trails Dr. The Woodlands TX 77381 USA.
- ²⁴ J. Dong, O. F. Sankey, and C. W. Myles, Phys. Rev. Lett. **86**, 2361 (2001).
- ²⁵ J. E. Graebner, B. Golding, and L. C. Allen, Phys. Rev. B **34**, 5696 (1986).
- ²⁶ R. O. Pohl, Phys. Rev. Lett. **8**, 481 (1962).
- ²⁷ S. Paschen, W. Carrillo-Cabrera, A. Bentien, V. H. Tran, M. Baenitz, Y. Grin, and F. Steglich, Phys. Rev. B **64**, 214404 (2001).